J. Plasma Physics (1998), *vol.* 59, *part* 1, *pp.* 69–82. Printed in the United Kingdom

© 1998 Cambridge University Press

Microwave coherent backscattering from acoustic or electronic waves in a magnetized plasma

FRANCESCA PISANI,[1] THIÉRY PIERRE[2] and DIMITRI BATANI[1]

[1] Università degli Studi di Milano, Dipartimento di Fisica. Via Celoria 16, 20133 Milan, Italy
[2] Université Nancy I, Laboratoire Physique Milieux Ionisés, URA 835 CNRS, BP 239, 54506 Vandoeuvre les Nancy Cedex, France

(Received 27 May 1996 and in revised form 17 December 1996)

A microwave coherent backscattering experiment has been carried out on Mirabelle, a weakly ionized plasma device, with the objective of measuring the electron-density fluctuation level. The experiment is a preliminary step in order to prepare the detection system for a microwave stimulated-backscattering experiment. The incident electromagnetic wave is focused in front of a plane grid, which excites ion acoustic or electron Bernstein waves and induces fluctuations in the plasma. The backscattering signal is collected by the launching circuit and detected by homodyne mixing. The typical ratio of the scattered power to the incident power is about 10^{-12} and the relative density fluctuations is of the order of $\delta n_e/n_e \approx 10^{-3}$ against a background electron density $n_e = (1\text{–}5) \times 10^9$ cm^{-3}. The backscattering measurement is also compared with Langmuir-probe measurements, and gives good agreement with the relative density fluctuations. The spectral width of the backscattered signal has also been studied, by taking into account effects due to the incident-wave focusing and plasma-wave damping.

1. Introduction

The scattering of electromagnetic waves from plasma is a very useful diagnostic for density or electron temperature. In fact, as in a generic continuous medium, the spectrum and the intensity of the scattered radiation, due to the density fluctuations that destroy the optical homogeneity of the medium, gives information about plasma properties (Sheffield 1975).

In our experiment we treat a case of coherent backscattering by the electron-density fluctuations associated with plasma waves in the ion acoustic or electron Bernstein frequency range.

Coherent scattering take place when the fluctuations have typical scale greater than the Debye length λ_{De} and they are associated with collective phenomena in the plasma.

The diagnostic method based on scattering offers some remarkable advantages. First of all, it is a non-perturbative method that only needs the accessibility of the radiation in the plasma (which implies for instance the choice $\omega_i > \omega_{pe}$). Furthermore, it allows one to investigate the inner zone of the

https://doi.org/10.1017/S0022377897006260 Published online by Cambridge University Press

plasma at higher electron density. This is particularly useful when hot plasma needs to be studied, and only investigation methods through wave or particle beams are possible. Hence backscattering diagnostics will be of special value for the study of hot and dense thermonuclear plasmas in the next generation of large tokamak device (Costley *et al.* 1988; Nizienko *et al.* 1993; Laviron *et al.* 1995).

Moreover, backscattering diagnostics have been widely used over the last twenty years in laser-produced plasmas. In this case, because of the high intensity of the electromagnetic beam (incident laser), the fluctuations are produced by the incident wave itself. We then speak about 'Stimulated' scattering (Giulietti *et al.* 1989; Rosenbluth and Sagdeev 1991; Gizzi *et al.* 1992). In this field, even after many years of study, many aspects need still to be clarified. The achievement of small-scale experiments on steady-state machines takes advantage of the temporally (and often spatially) flat plasma profiles. Some nonlinear wave experiments have already been realized on Mirabelle (Pierre 1990; Bonhomme *et al.* 1991).

Hence the objective of our experiment was twofold: first to study electromagnetic scattering from a plasma and secondly as a preliminary experiment towards the realization of a plasma diagnostic based on stimulated scattering and to provide a calibration of the detection system for such an experiment.

Both stimulated and 'normal' scattering of electromagnetic waves are constrained by selection rules (or 'phase-matching' conditions) representing the energy and momentum conservation in the interaction between the incident and the plasma wave. In the case of backscattering, the scattering angle is 180°. If, moreover, $\omega_i \gg \omega_f$, the selection rules simply become

$$\omega_s \approx \omega_i, \tag{1.1a}$$

$$|\mathbf{k}_f| \approx 2|\mathbf{k}_i|, \tag{1.1b}$$

where the indices s, i and f refer to the scattered, incident and fluctuation waves respectively, which implies $\lambda_i \approx 2\lambda_f$. Therefore, in order to produce backscattering, it is then necessary to excite in the plasma a wave with wavelength λ_f half of the incident wavelength λ_i.

By measuring the scattered power P_s, we can find the value of the fluctuating electron density δn_e, through the following approximate (see the appendix) formula:

$$P_s = P_i(\lambda_i r_0 L\, \delta n_e)^2, \tag{1.2}$$

where L gives the linear dimensions of the 'scattering' volume, i.e. the plasma volume where the interaction between the incident wave and the plasma wave takes place, P_i and λ_i are the power and the incident wavelength respectively, and $r_0 = 2.8 \times 10^{-13}$ cm is the classical electron radius.

2. Experimental set-up and practical conditions of measurement

The experiment was carried out on Mirabelle, a magnetized double-plasma device, described elsewhere (Pierre *et al.* 1987) and shown in Fig. 1.

The device consists of two identical cylindrical chambers (diameter 1 m and length 1 m) connected by a central horizontal column (diameter 30 cm and length 1.4 m).

https://doi.org/10.1017/S0022377897006260 Published online by Cambridge University Press

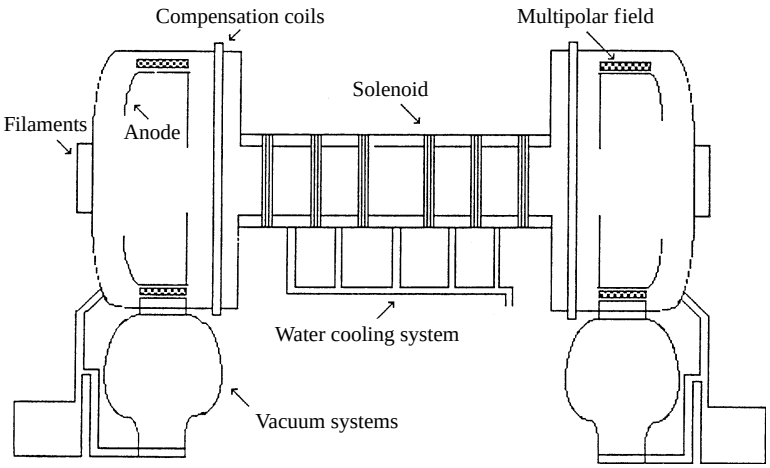


Figure 1. Schematic of the Mirabelle device.

Table 1. Parameters of the Mirabelle plasma

n_e	$(1–5 \times 10^9$ e cm^{-3}
T_e	1–6 eV
ω_{pe}	640 MHz
λ_{De}	0.3 mm
ω_{pi}	7.47 MHz (He), 2.48 MHz (Ar)

The plasma is produced by an electrical discharge in a low-pressure gas ($P \approx 10^{-4}$ Torr) in the large vacuum chamber, where a series of tungsten filaments, located at the end of the end-chambers, emit the ionizing primary electrons, creating a diffusion plasma.

The magnetic confinement system consists of a solenoid wrapped around the central column and of two multipolar magnetic fields at the walls of the lateral chambers, which have the task of reflecting the primary electrons and pushing them towards the column. The reflection at the walls also provides a randomization of the electron trajectories. Consequently, these fields ensure the presence of a relatively dense and uniform plasma, especially in the central zone of the device.

Two values of the magnetic field were used during the experiment: a 'low' field ($B \approx 60$ G) and a 'high' field ($B \approx 200$ G).

With an electron density $n_e = 5 \times 10^9$ cm^{-3} and a typical neutral density $n_a \approx (1–3) \times 10^{11}$ cm^{-3} (corresponding to a pressure $P \approx 10^{-4}$ Torr), the average degree of ionisation $Z^* = n_e/n_a$ is about 3%; hence the plasma of Mirabelle is just weakly ionized.

The device works with helium or argon with the typical parameters shown in Tables 1–3. Because the low degree of ionization, energy transfer between ions and electrons is very poor, leaving a cold ion population at $T_i \approx 0.025–0.1$ eV (the first value has been used to calculate the ion Larmor radii in Tables 2 and 3).

T_e and n_e were measured by means of a Langmuir probe with a circular surface 6 mm in diameter. The probe was oriented perpendicularly to the magnetic field lines in the column: this allows only an axial measurement of

https://doi.org/10.1017/S0022377897006260 Published online by Cambridge University Press

Table 2. Mirabelle plasma in $B = 60$ G.

Ω_e	170 MHz
ρ_{Le}	0.56–0.79 mm
Ω_i	45 Hz (He), 41 Hz (Ar)
ρ_{Li}	11 mm (He), 34 mm (Ar)

Table 3. Mirabelle plasma in $B = 200$ G.

Ω_e	560 MHz
ρ_{Le}	0.16–0.23 mm
Ω_i	151 Hz (He), 137 Hz (Ar)
ρ_{Li}	3.2 mm (He), 10 mm (Ar)

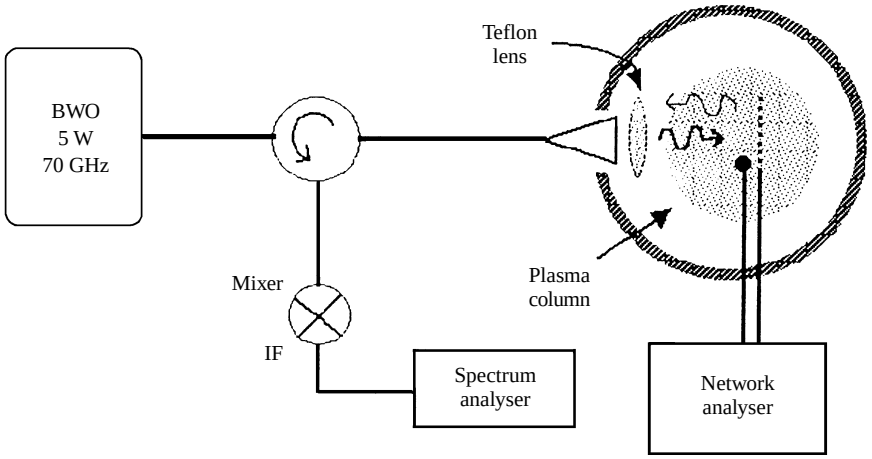


Figure 2. Experimental set-up.

plasma parameters. In fact, the measurement of the electron current is very sensitive to the probe orientation with respect to the magnetic field lines, as the electrons are strongly magnetized (typically, we had $\rho_e \approx 0.1$–0.8 mm, depending on experimental conditions).

Such a strong magnetization was taken into account in Langmuir-probe measurements (since it brings about a strong reduction in the electron saturation current owing to limitation of the electron motion around the magnetic lines in the direction perpendicular to the field) (Batani *et al.* 1996).

The T_e measurement is less sensitive to the probe orientation in the magnetic field, because it is based on the electron energy discrimination and not on the quantity of electrons collected by the probe. The typical reliability of the parameters measured with the Langmuir probe was about 20 %.

The general experimental set-up used for backscattering is shown in Fig. 2. It consists of a launching circuit for the incident electromagnetic wave, a circuit for the detection of the scattered wave and an excitation–detection system for plasma waves. As scattering is at 180°, the launching circuit and the detection circuit were lumped together in just one compact circuit located laterally outside the column of Mirabelle.

https://doi.org/10.1017/S0022377897006260 Published online by Cambridge University Press

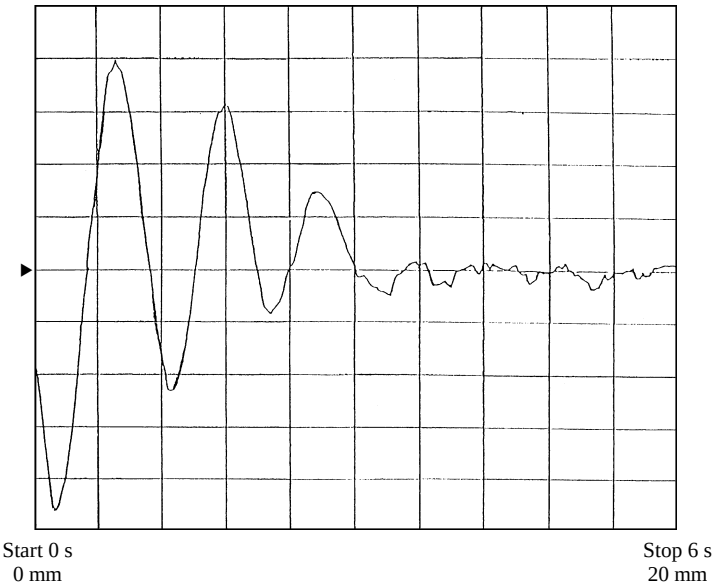


Figure 3. A typical interferogram of an ion acoustic wave excited at $f = 2$ MHz, showing a wavelength $\lambda = 3.4$ mm in a helium plasma.

The incident wave was generated by BWO ($\lambda_i = 4.28$ mm, $k_i = 1468$ m^{-1}, $P_i = 5$ W and $f_i = 70$ GHz); hence, with $n_e = 5 \times 10^9$ cm^{-3}, $\lambda_i = 4.28$ mm and $T_e = 2$ eV, the Salpeter parameter is $\alpha \approx 1.76$, so we have the case of $\alpha \approx 1$.

The incident wave passes through a circulator: a small part is transmitted towards a mixer while the greatest part is injected into the plasma column through a horn antenna and focused in the interaction zone by means of a Teflon lens.

The plasma scattered wave is collected by the same antenna through the circulator, and transmitted to the mixer, where it is detected by homodyne detection, i.e. the backscattered signal is mixed with a reference signal (in our case a small part of the incident wave). Hence the mixer output signal is a wave with frequency given by the difference between the mixed wave frequencies (ω_i and ω_f) and power given by the backscattered power: this signal is then sent to the spectrum analyser.

The received signal has a very low power, owing to attenuation on passing through the plasma and in the waveguide. Therefore, in order to use this microwave circuit for the detection of backscattering, it is necessary to calibrate the circuit itself to determine the minimum detectable power (before it is covered by the noise). With this aim, we simulated the backscattered signal by a second microwave source, a klystron with $f \approx 71$ GHz and $P \approx 300$ mW, and we found that the minimum detectable is about -85 dBm.

The excitation–detection system for the plasma waves was a network analyser, which supplies a plane grid parallel to the magnetic field. At the same time, a simple moving probe, in front of the grid (able to detect a plasma volume 20 mm long and wide), collects the wave signal in the plasma and transmits it to the network analyser, which generates an interferogram. A typical record is shown in Fig. 3; this corresponds to an ion acoustic wave

https://doi.org/10.1017/S0022377897006260 Published online by Cambridge University Press

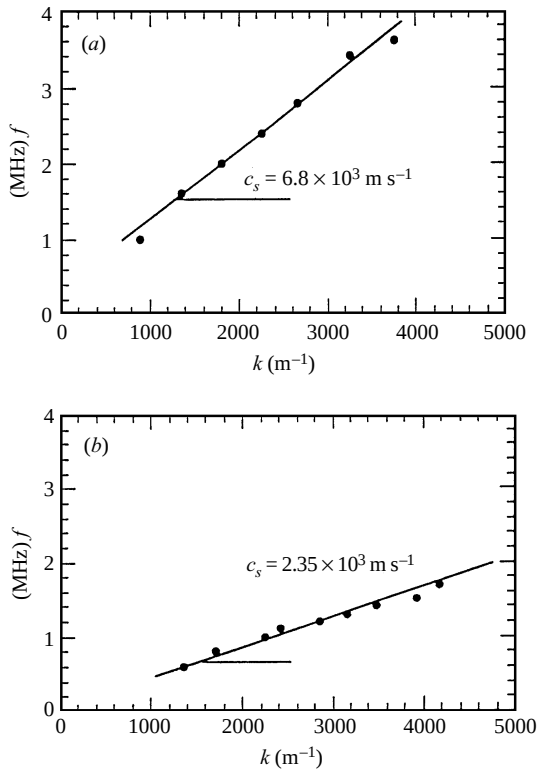


Figure 4. Experimental ion acoustic dispersion relation showing the linear trend expected in the low-magnetic-field approximation ($B \approx 60$ G): (*a*) for helium; (b) for argon.

obtained in a helium plasma at 2 MHz frequency. We can directly measure the wavelength of the wave excited in the plasma; here it is $\lambda_f = 3.4$ mm.

By recording such interferograms at different wave frequencies, it is possible to reconstruct the dispersion relation of the wave in the plasma. We have obtained this in both helium and argon plasmas, and for both ion acoustic and electron Bernstein waves.

The ion acoustic dispersion relation is shown in Fig. 4. This was obtained with $B \approx 60$ G (which corresponds to an ion cyclotron frequency $\Omega_i = 40$–50 kHz), and allows us to consider the low-magnetic-field approximation $\omega_{ia} \gg \Omega_i$, when the frequency of the ion acoustic waves ω_{ia} is in the range 1–4 MHz. In this case the dispersion relation is simply given by (Chen 1974)

$$\omega_{ia} = c_s k. \tag{2.1}$$

Here c_s is the sound velocity, given by ($T_i \ll T_e$)

$$c_s = \left(\frac{k_B T_e}{M_i}\right)^{1/2}, \tag{2.2}$$

where k_B is the Boltzmann constant, M_i the ion mass and T_e the electron temperature. Figure 4 shows clearly the linear trend expected from the theoretical dispersion relation.

https://doi.org/10.1017/S0022377897006260 Published online by Cambridge University Press

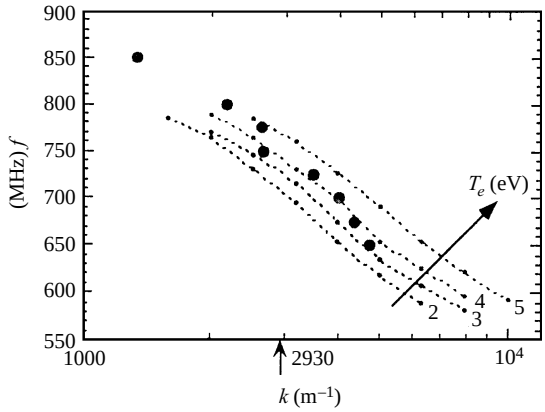


Figure 5. Electron Bernstein dispersion relation (for argon and $B \approx 200$ G). The points indicate the experimental data and the four lines the computational results at four different values of T_e: 2, 3, 4 and 5 eV.

From the slope of the experimental curve, we can find the sound velocity: $c_s = 6.8\%10^3$ m s^{-1} for helium and $c_s = 2.35 \times 10^3$ m s^{-1} for argon. By means of (2.2), we obtain the values of the electron temperature: $T_e = 2$ eV in helium and $T_e = 2.4$ eV in argon. The slight difference between these values and from those obtained with a Langmuir probe are probably due to the plasma anisotropy resulting from the presence of the magnetic field.

The study of the dispersion relation of plasma waves in very important for the determination of the practical conditions of measurement, as imposed by the phase-matching rules. With a 4.3 mm incident wavelength, we must excite 2.15 mm wavelength plasma waves, which correspond to a wave vector $k = 2936$ m^{-1}. The frequency values found, with an error of about 10 % due to the interpolation of the experimental data, are

$$\text{helium} \qquad 3.1 \text{ MHz} \pm 0.3 \text{ MHz}; \tag{2.3a}$$

$$\text{argon} \qquad 1.2 \text{ MHz} \pm 0.12 \text{ MHz}. \tag{2.3b}$$

Figure 5 shows the dispersion relation for electron Bernstein waves (Pierre *et al.* 1989) obtained for an argon plasma in a magnetic field $B \approx 200$ G. This value of B corresponds to a electron cyclotron frequency $\Omega_e = 560$ MHz and, with a plasma frequency $\omega_{pe} = 640$ MHz, gives an upper-hybrid frequency

$$\omega_{uh} = (\omega_{pe}^2 + \Omega_e^2)^{1/2} = 850 \text{ MHz}. \tag{2.4}$$

Hence we have the $\omega_{uh} < \Omega_e$ case, and we can reconstruct the branch of the dispersion relation between Ω_e and ω_{uh}.

The desired frequency producing backscattering ranges between 700 and 750 MHz. Figure 5 shows the experimental data compared with the computational results at four different values of E_e. Comparison with experimental data also offers an efficient method for estimating the electron temperature. In fact, experimental data are included in the range between 3 and 5 eV, in good agreement with Langmuir-probe measurements.

As shown in Fig. 3, the ion acoustic waves generated by the plane grid are strongly damped as they propagate through the plasma, with a typical damping length L_{pl} of the order of 1 cm.

https://doi.org/10.1017/S0022377897006260 Published online by Cambridge University Press

By interpolating the experimental points in each interferogram with an oscillation at frequency ω_f with a decreasing exponential envelope like

$$\phi(r) = A_0 \cos(k_f r) \exp\left(-\frac{|r|}{L_{pl}}\right), \tag{2.5}$$

where A_0 is the wave amplitude and r the distance from the grid, we can obtain a damping length L_{pl} of about 0.5 cm. This value is important just in order to obtain an order of magnitude for the length L_{pl}.

We note that the phase velocity of the wave, $c_s \approx 10^3$ m s^{-1}, is much greater than the ion thermal velocity ($v_{T_i} = (k_B T_i/M_i)^{1/2} \approx 20$–$50$ m s^{-1} in argon and ≈ 700–1500 m s^{-1} in helium, with a ion temperature T_i from 0.025 eV to 0.1 eV). Furthermore, this phase velocity is much less than the electron thermal velocity ($v_{Te} = (k_B T_e/m_e)^{1/2} \approx 6 \times 10^5$ m s^{-1} with electron temperature $T_e \approx 2$ eV), and consequently the ions see an almost 'flat' electron distribution. These two conditions exclude Landau damping both for ion and electron waves. Hence damping must essentially be due to collisional effects.

We also note that, even if the plasma is weakly ionized, the dominant types of collisions are those between charged particles. Indeed, with typical values $T_i = 0.025$ eV and $T_e = 2$ eV, we get

$$\nu_{i-n} = n_e 4\pi r_{at}^2 v_{T_i} \approx 2 \text{ Hz}, \tag{2.6a}$$

$$\nu_{e-e} = 2.92 \times 10^{-6} n_e \ln\Lambda\, T_e^{-3/2} \approx 2.5 \times 10^4 \text{ Hz}, \tag{2.6b}$$

$$\nu_{i-i} = 4.8 \times 10^{-8} n_i Z^2 \ln\Lambda\, T_i^{-3/2} \approx 2.4 \times 10^6 \text{ Hz}, \tag{2.6c}$$

where ν_{i-n}, ν_{e-e} and ν_{i-i} are respectively the ion–neutral, electron–electron and ion–ion collision frequencies, and $\ln\Lambda \approx 20$–25 is the Coulomb logarithm.

Hence we can estimate the damping length L_{pl} by means of the dispersion relation by taking into account only the ion–ion collision term. The collisional dispersion relation is

$$\omega_{ia}^2 - c_s^2 k^2 = -\frac{i\omega}{\tau}, \tag{2.7}$$

where $\tau = 1/\nu_{i-i}$ is the characteristic collision time.

The damping length is given by the imaginary part of the wave vector, obtained, in the approximation $\nu_{i-i}/\omega_{ia} < 1$, as

$$L_{pl} = \frac{1}{\text{Im}(k)} \approx \frac{2c_s}{\nu}. \tag{2.8}$$

With $c_s = 6.8 \times 10^3$ m s^{-1} (in helium) and with a wave frequency from 1 MHz up to a maximum of 4 MHz, we finally find L_{pl} varying from about 0.5 cm to about 2 cm, in good agreement with the value obtained from numerical interpolation of the experimental interferogram.

3. Backscattering results

The backscattering signal has been obtained with the ion acoustic wave in both helium and argon plasmas. Figure 6(*a*) shows such a backscattering signal as a function of the plasma wave frequency for the case of a *helium* plasma.

Because the study of the dispersion relation of the plasma waves gave us only the frequency range (2.3), it was necessary to make a final fine adjustment of

https://doi.org/10.1017/S0022377897006260 Published online by Cambridge University Press

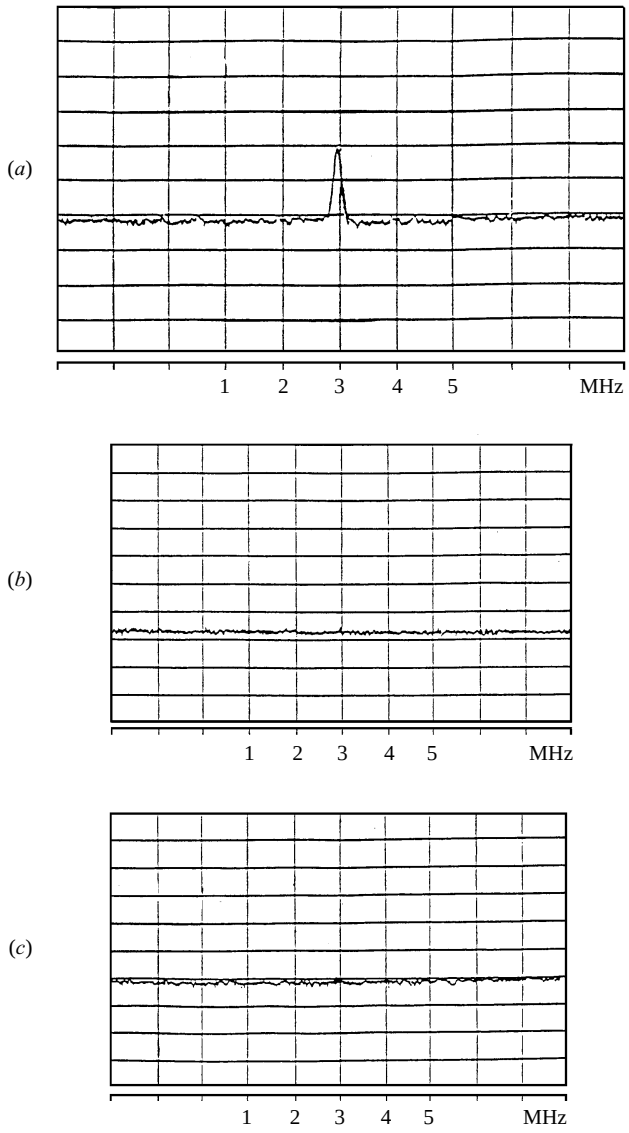


Figure 6. Backscattering signal obtained in a helium plasma with ion acoustic waves (*a*). The maximum frequency $f_{\max} = 2.897$ MHz indicates the exact resonance condition. We can observe the signal dropping to the noise level with no microwave source (*b*) and by switching off the discharge (*c*).

the grid-exciting frequency to satisfy the phase-matching rules and obtain a backscattered peak of maximum intensity.

We also checked, through some experimental tests, that the peak was really due to backscattering (this was particularly important because of the risks of interference caused by poor shielding of the detection system). As shown in Figs 6(*b*, *c*), with no microwave source the peak dropped to the noise level, confirming that it did not correspond to a parasitic signal generated by the supply system of the BWO. Similarly, by switching off the discharge, we stopped plasma production, and again the peak dropped.

https://doi.org/10.1017/S0022377897006260 Published online by Cambridge University Press

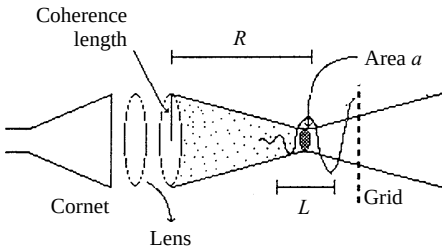


Figure 7. Scheme showing the geometry of the interaction process between an incident electromagnetic beam and plasma waves excited by the grid.

The frequencies corresponding to the maximum intensity of the observed peak were $f_{\max} = 1.35$ MHz for argon and $f_{\max} = 2.9$ MHz for helium – values that fall in the expected range (2.3). This is further proof that the observed signal is caused by plasma scattering fluctuations in the acoustic range.

In both cases of helium and argon, the scattered power was about 100 dBm, corresponding to an effective value of about -85 dBm when taking into account the circuit attenuation of about -25 dB. The typical value of the ratio of scattered to incident power was hence about 10^{-12}.

To find the electron-density fluctuation δn_e, we use (1.6) and assume L to be the length of the zone where the focused incident electromagnetic wave and the plasma wave coexist (and hence scattering take place), as shown in Fig. 7.

Hence L can be estimated as the minimum between the plasma-wave damping length, obtained from the experimental interferograms (Fig. 3), and the depth of focus (Klein and Furtak 1986) of the incident electromagnetic beam. The latter is equal to $L_F = 3.9f^2\lambda_i/b^2$ for a diffraction-limited beam (where f and b are respectively the focal length and the lens diameter and, in our case, $f/b \approx 1.6$). Thus

$$L = \min [L_{pl}, L_F]. \tag{3.2}$$

For our conditions, $L_F \approx 4$ cm and $L_{pl} \approx 1$ cm.

Finally, from (1.6), we obtain a relative electron-density fluctuation of

$$\delta n_e / n_e \approx 10^{-3} \tag{3.3}$$

(when the electron density $n_e = 5 \times 10^9$ cm^{-3}). This value is in good agreement with the measurements obtained using the Langmuir probe, as described in the following section.

Technical problems appeared in the Raman backscattering experiment due to the presence of a parasitic signal generated by direct excitation by the grid of an electromagnetic wave at the same frequency as the detection frequency. Hence an alternative method for Raman backscattering would be to choose a plasma regime in which the possibility of coupling between the electromagnetic wave excited by the grid and the detector can be avoided; this is obtained by changing the plasma density and the magnetic field (Bonhomme 1989).

4. Direct measurement by Langmuir probe

The measurement of the fluctuations δn_e created in the plasma by the excitation of plasma waves can be conducted, in the case of ion acoustic waves, in a 'direct' way by means of a Langmuir probe.

In fact, the density fluctuation induces a fluctuation in the electron

https://doi.org/10.1017/S0022377897006260 Published online by Cambridge University Press

saturation current $I^-_{\rm sat}$ collected by the probe, the two being directly proportional. As a consequence, $I^-_{\rm sat}$ is the sum of the two contributions: the first represents an average where fluctuations cancel each other and coincides with the current measured in a unperturbed plasma; the second is due to an alternating current that oscillates at the wave frequency ω_f:

$$I^-_{\rm sat} = I^- + \delta I^-. \tag{4.1}$$

At low frequencies (for ion acoustic waves), the following approximation holds:

$$\frac{\delta n_e}{n_e} = \frac{\delta I^-}{I^-}. \tag{4.2}$$

We measured $\delta I^-/I^- = 3\times 10^{-3}$, with a typical current $I^- = 0.3$ mA. Hence, by measuring the relative fluctuation of the current, we find the relative fluctuation in the density:

$$\frac{\delta n_e}{n_e} = 3\times 10^{-3}, \tag{4.3}$$

which is in quite good agreement with the value found through the backscattering measurement, and confirms the validity of our measurement method.

5. Peak width

Figure 6 shows that the backscattered signal has a frequency width of about 0.2 MHz. This can be due to several causes, including the spectral width of the source, the resolution of the spectrum analyser, the optical focusing spread of the incident wave, or the spectral width of the plasma wave due to its damping. In our case the first two cases are negligible, being of the order of 10 Hz; we now examine the other two in detail.

(i) As a result of focusing of the incident beam, the incident wave vector $\mathbf{k}_i$ does not have a fixed direction, but can make an angle θ with the plasma wave vector $\mathbf{k}_f$, which is perpendicular to the grid. The uncertainty about the direction of $\mathbf{k}_i$ becomes, through the selection rules, an uncertainty in the resonance condition, and consequently in the scattered wave and in the direction of wave vector $\mathbf{k}_d$ (see Fig. 8).

Then we can estimate the contribution to the peak width due to focusing geometry, using the selection rules for $\mathbf{k}$. By decomposition along the directions parallel and perpendicular to the normal to the grid, the selection rules become

$$k_f = k_i\cos\theta - k_d\cos\phi, \tag{5.1a}$$

$$0 = k_i\sin\theta - k_d\sin\phi, \tag{5.1b}$$

where θ and ϕ are the angles formed by the vectors $\mathbf{k}_i$ and $\mathbf{k}_s$ respectively. These two angles vary between 0° and $\theta_{\rm max}$, where $\theta_{\rm max}$ coincides with the focusing spread angle determined by the ratio f/b (for our conditions, $\theta_{\rm max}\approx 17°$).

From (5.1), we find

$$\phi = \frac{k_i\sin\theta}{k_i\cos\theta - k_f}, \tag{5.1a}$$

$$k_d = \frac{k_i\cos\theta - k_f}{\cos\phi}. \tag{5.2b}$$

https://doi.org/10.1017/S0022377897006260 Published online by Cambridge University Press

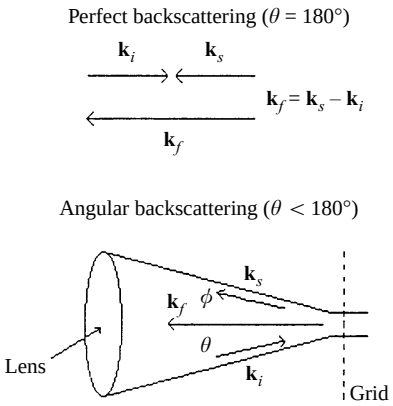


Figure 8. Geometry of selection rules for wave vectors.

From (5.2a), we have $\phi_{\max} \approx 16.4°$ as the maximum angle of the scattered radiation. By substitution into (5.2b), we finally get $\mathbf{k}_d = 1635\ \mathrm{m}^{-1}$, corresponding to the angle $\phi_{\max}$.

Therefore the variation in k_s is $\Delta k_s = k_2(\phi = 0°) - k_s(\phi = 16.4°) = 139\ \mathrm{m}^{-1}$. This width in k corresponds to a width in the frequency of the detected signal of about $\Delta f_1 \approx 0.11$ MHz.

(ii) The damping of the plasma wave propagating from the grid in the plasma also contributes to the spectral width of the scattered wave.

By making the Fourier transform $\tilde{\phi}(k)$ of (2.5), we find the power spectrum of the plasma wave $G(k) = \tilde{\phi}\tilde{\phi}^*$ to be given by

$$G(k) = \frac{A_0^2}{4[(k-k_f)^2 + (2/L_{pl})^2]}. \tag{5.3}$$

This is maximum for $k = k_f$, and the half-value is obtained when $k = k_f \pm 2/L_{pl}$. The width is then $\Delta k_f = 4/L_{pl}$.

Finally, we have $\Delta k_s/k_s = \Delta k_f/k_f$, from which we find, with a damping length of the order of $L_{pl} \approx 1$ cm, a frequency width of the scattered signal $\Delta f_2 \approx 0.43$ MHz.

The total width, due both to focusing and to damping effects, is

$$\Delta f_{\mathrm{tot}} = [(\Delta f_1)^2 + (\Delta f_2)^2]^{1/2} \approx 0.44\ \mathrm{MHz}. \tag{5.4}$$

This is greater than the experimental value of about 0.2 MHz, but it is of the same order of magnitude. Hence we believe that the observed width of the backscattering signal is really due to a geometrical focusing effect plus damping of the excited waves in the plasma.

6. Conclusions

We have measured the electron-density fluctuation in the weakly ionized plasma of Mirabelle, with a backscattering experiment where the density fluctuations are induced in the plasma by an external cause (by excitation of ion acoustic or electron Bernstein waves).

https://doi.org/10.1017/S0022377897006260 Published online by Cambridge University Press

The maximum backscattering intensity corresponds to a resonance condition imposed by the phase selection rules, when the wavelength associated with plasma fluctuations is half of the incident wavelength. The resonance wavelength corresponds to what is expected on the basis of the study of the dispersion relation of plasma waves. The scattered power measurement gave a value of -85 dBm, corresponding to a relative density fluctuation $\delta n_e/n_e \approx 10^{-3}$, also confirmed by comparison with Langmuir-probe measurements in the low-frequency range. Moreover, this check allowed us to calibrate our experimental apparatus in view of a future experiment on plasma diagnostics using stimulated backscattering. For such an experiment, a much larger electromagnetic incident intensity is needed for the same plasma conditions in order to generate a fluctuation level greater than noise.

Acknowledgements

This work was partly funded through the European Union Contract CHRX-CT93-0356 (HCM Network on 'Non linear phenomena in microphysics of collisionless plasmas'). Francesca Pisani participated in the experiment thanks to an ERASMUS Grant obtained in the framework of the PIC coordinated by Professor L. Lanz (University of Milan). Finally, we should like to warmly thank Dr M. Lontano (IFP, CNR, Milan) and Professor F. De Luca (University of Milan) for useful discussions and their kind interest in our work.

Appendix

The scattered power in the frequency unit is given by (Sheffield 1975)

$$dP_s = d\omega\, d\Omega\, \varepsilon_0\, c|\mathbf{u}\times\mathbf{E}_i|^2\, r_0^2 \left(\frac{\omega_s}{\omega_i}\right)^2 \bar{n}_e\, VS(\omega,\mathbf{k}), \tag{A 1}$$

and, by integration over frequency, we obtain

$$dP_s = d\Omega\, P_i\, r_0^2 \left(\frac{\omega_s}{\omega_i}\right)^2 \bar{n}_e \frac{V}{a} S(\omega,\mathbf{k}), \tag{A 2}$$

where the incident power P_i is given by

$$P_i = \int \varepsilon_0\, c|\mathbf{E}_i|^2\, a\, d\omega. \tag{A 3}$$

Here V is the scattering volume, already defined, and a represents the transverse area of this plasma zone and coincides with the focal spot of the incident beam (with our focusing optics, its diameter is $\rho = 1.22\lambda_i/b \approx 7.7$ mm, which is of the order of the grid size). Since density fluctuations and the incident wave are important only in the volume V, we can associate the fluctuations with a group of waves with extension of the order V. The fluctuation $\tilde{n}(\mathbf{r},t)$, defining the spectral-density function $S(\omega,\mathbf{k})$, may then be given by the Fourier transform

$$\tilde{n}(\mathbf{r},t) = \int d^3\mathbf{k}\, \tilde{n}(\omega,\mathbf{k})\, e^{i\mathbf{k}\cdot\mathbf{r}}, \tag{A 4}$$

and $\tilde{n}(\omega,\mathbf{k})$ also assumes a Gaussian form with width $\Delta k = 1/V$.

https://doi.org/10.1017/S0022377897006260 Published online by Cambridge University Press

After normalization, we find a normalization coefficient given by $1/\Delta k = V$.

Finally, it has been shown (Slusher and Surko 1980) that the connection between the spectral density function S and the fluctuation density is given by

$$s = V\frac{\langle|\tilde{n}|^2\rangle}{\bar{n}_e}. \tag{A 5}$$

Because the scattering is at 180°, we can identify the scattering solid angle $d\Omega$ with the coherence angle of emitted radiation, which is given by:

$$\Delta\Omega = \frac{A}{R^2}, \tag{A 6}$$

where R is the observation distance and A is the solid-angle area. If $l = \lambda R/\pi\rho$ is the coherence length and ρ is the radius of the focal spot then the area A is

$$A = \pi|^2 = \pi\left(\frac{\lambda R}{\pi\rho}\right)^2, \tag{A 7}$$

and finally the solid angle is given by

$$\Delta\Omega = \frac{\pi\lambda^2R^2}{R^2\pi^2\rho^2} = \frac{\lambda^2}{\pi\rho^2} = \frac{\lambda^2}{a}. \tag{A 8}$$

Hence, by integration of (A 2) over the calculated solid angle and by assuming that $\omega_s \approx \omega_i$, we obtain a simple formula giving the relation between the total scattered power and the fluctuation δn_e, when λ_i, P_i and L are known:

$$P_s = P_i(\lambda_i r_0 L\,\delta n_e)^2 \tag{A 9}$$

References

Batani, D., Alba, S, Galassi, A. and Lombardi, P. 1996 *Vuoto* **25**, 81.

Bonhomme, G. 1989 Thèse d'Etat, University of Nancy.

Bonhomme, G., Pierre, Th., Leclert, G. 1991 *Plasma Phys. Contr. Fusion* **33**, 507.

Book, D. L. 1987 *NRL Plasma Formulary*. Naval Research Laboratory, Washington, DC.

Costley, A. E. *et al.* 1988 *JET Report* JET-R(88)08, Culham.

Chen, F. F. 1974 *Plasma Physics*. Plenum Press, New York.

Giulietti, A., Giulietti, D., Batani, D. *et al.* 1989 *Phys. Rev. Lett.* **63**, 524.

Gizzi, L., Batani, D., Biancalana, V. *et al.* 1992 *Laser Interaction and Related Plasma Phenomena*, Vol. 10 (ed. H. Hora and G. H. Miley). Plenum Press, New York.

Klein, M. and Furtak, T. 1986 *Optics*. Wiley, New York.

Laviron, C., Millot, P. and Prentice, R. 1995 DRFC/CAD, EUR-CEA-FC-1541.

Nielsen, P. *et al.* 1993 *JET Report* JET-P(93)62, Culham.

Nizienko, Yu. *et al.* 1994 *Rev. Sci. Instrum.* **65**, 2460.

Pierre, Th. 1990 *Europhys. Lett.* **11**, 139

Pierre, Th., Leclert, G. and Braun, F. 1987 *Rev. Sci. Instrum.* **58**, 6.

Pierre, Th., Leclert, G. and Braun, F. 1989 *Phys. Rev. Lett.* **62**, 1627.

Pisani, F. 1995 Laurea thesis. University of Milan.

Rosenbluth, M. and Sagdeev, R. 1991 *Handbook of Plasma Physics*, North-Holland, Amsterdam.

Salpeter, E. E. 1960 *Phys. Rev.* **120**, 1528.

Sheffield, J. 1975 *Plasma Scattering of Electromagnetic Radiation*. Academic Press, New York.

Slusher, R. E. and Surko, C. M. 1980 *Phys. Fluids* **23**, 472.

https://doi.org/10.1017/S0022377897006260 Published online by Cambridge University Press